Absorption cross section of building materials at mm wavelength in a reverberation chamber

D. Micheli[(1)], A. Delfini[(2)], R. Pastore[(2),] Mario Marchetti[(2)], R. Diana[(3)], G. Gradoni [(4)]

[(1)] Telecom Italia S.p.A. Operations Engineering & TILab Wireless Access Engineering & Devices,
Via di Val Cannuta 250, 00166 Roma, Italy.
Email: davide.micheli@telecomitalia.it
[(2)] Astronautics, Electric and Energy Engineering Department (DIAEE), 'Sapienza' University of Rome,
Via Eudossiana 18, 00184 Roma, Italy.
Email: andrea.delfini@uniroma1.it, roberto.pastore@uniroma1.it, mario.marchetti@uniroma1.it
[(3)] Anritsu, Via Sante Bargellini, 4, 00157 Roma, Italy.
Email: roberto.diana@anritsu.com
[(4)]University of Nottingham: School of Mathematical Sciences
University Park Nottingham, UK.
Email: gabriele.gradoni@nottingham.ac.uk

ABSTRACT

The reverberation chamber method is used to estimate the average absorption cross section of building materials at mmWave frequencies. Analysed samples include concrete, bricks of different types, and wood. The investigation is carried out in the frequency range between 50 GHz and 68 GHz, which is of interest in the next generation of mobile telecommunication system. A cylindrical cavity is transformed into a reverberation chamber through the use of a mechanical model stirrer. The chamber field is statistically homogeneous and depolarized; therefore it can be used to probe the average response of the sample under test. In particular, through a differential measure of the average quality factor (average insertion loss) it is possible estimate the fraction of power absorbed by the sample under test. Several cube-shape samples have been characterized and compared. Obtained results show that analysed samples have remarkably different levels of the electromagnetic wave absorption, depending on both material density and chemical composition. The absorption of pure water is used as a baseline to determine the dynamic range of the measurement.

Keywords: 5G, millimeter frequencies, absorbing cross section, reverberation chamber, building materials

1 INTRODUCTION

The next generation of mobile networks will make use of millimeter frequency bands. At those frequencies, the electromagnetic (EM) wave propagation mechanisms must be characterized and understood. This is very important in the planning of city coverage of wireless signals. In the urban environment and inside buildings, the absorption of EM energy caused by building materials needs to be properly characterized. The operation frequencies of the 5G networks have not yet been defined. However, referring to preliminary studies on mm Wave Propagation [1,2], a systematic analysis of materials in the broad range from 50 GHz to 68 GHz is believed to be valuable.

Several experimental set-up are currently employed to characterize materials at mm wavelength. The main methods of measurement are based on waveguide, free space or resonant cavity systems, in a variety of configurations [3-8]. Nevertheless, such methods are not the most appropriate for a reliable characterization of building materials, which typically present irregular shape, random porosity and lack of homogeneity. In fact, waveguide methods have sample dimension strict constraints that may cause EM leakage problems, while free space measurements often suffer of unwanted edge effects; on the other hand, resonant cavity systems investigate materials behavior at isolate frequencies or in restricted range mainly. Moreover, the proposed task requires an analysis of realistic EM propagation environments. Although permittivity and permeability are intrinsic properties of the materials, the absorption capability of relatively large objects depends also on shape, volume, material type, and on the incoming wave polarization and direction of incidence. In real environment the excitation of any structure exhibits random characteristics: hence, evaluating the absorption capability for a particular condition could be meaningless. Therefore, a full characterization of EM absorption properties requires the measurement repetition using several angles of incidence and polarization. In particular, indoor propagation channels are characterized by multipath. Although most related research has dealt with path loss and temporal characteristics (such as time of arrival and delay spread), less attention has been paid to angle of arrival of multipath , which is crucial for predicting the performance of adaptive array systems. For these reasons, a reverberation chamber set-up [9-12] is believed to be the most suitable system to perform a realistic testing of building materials. Such instrumentation, in fact, allows to excite the material under test in a completely random way over a relatively broad frequency range, thus overcoming the limitation of other measurement methods based on transmission line models.

In this work, we perform an experimental evaluation of the average absorption cross section (ACS) of several building materials in reverberation chamber (RC). A well-established RC method [13-16] is used to investigate the absorption of material samples made of travertine, concrete, Roman brick and refractory

brick. The average absorption is of fundamental importance to predict the statistical field behavior, often showing field/power fluctuations and fading in indoor and outdoor electromagnetic environments (EME). It is a crucial input parameter for example in the statistical analysis of an RC [17,18], and in the Random Coupling Model (RCM) [19]. The paper is organized as follows: in section 2 the materials analyzed and the methods employed are reported, in section 3 the experimental results are presented and discussed, section 4 is then devoted to conclusions and highlights of research activity future developments.

2 MATERIALS AND METHOD

2.1 Materials under test

The materials under test are of common use in the construction of buildings. In particular, the following samples have been considered: a common brick made with ancient roman techniques (Roman Brick), which has been subjected to sandblasting (then called S); a Roman Brick not subjected to sandblasting (then called NS), which presents a different aspect, less smooth than the former; two kind of refractory bricks, called as Refractory Red (more smooth) and Refractory White (less smooth); a sample of ultra-light concrete, called as White Concrete; a Travertine sample, very commonly used in both ancient and modern architecture. The sample geometry is cubic with sides of about 5cm. An additional absorption measurement has been performed on a cylindrical polystyrene sample holder, with approximately the same volume of the cubic samples, filled up with 125 mL of demineralized water. Table 1 reports the density of the materials under test. Material density, as sample geometry, is believed to have a significant impact on the average quality factor (Q) [20,21], and therefore on the average ACS. Also the chemical composition of the materials is relevant in the absorption of electromagnetic waves, hence an appropriate analysis of the chemical characteristics of the materials under test has been performed. Specifically, White Concrete is porous and presents no aggregate larger than Quartz sand, which is typically used as binding agent (Aluminum powder is also inserted at a rate of 0.05%–0.08% by volume); it has lightweight and great resistance to fire. Roman Brick is a ceramic material made with purified clay, which is then pressed and cured in ovens. Both the Roman Bricks specimens present the same chemical composition, whereas the different density values are the result of different pressing manufacturing and curing. The refractory bricks are made of Clay, Calcium, with presence of alumina (Al_2O_3) and silica (SiO_2), and present a great resistance to fire; as for the Roman Bricks, the samples present same chemical composition and different density due to different manufacturing process. Finally, Travertine, that is a

sedimentary rock, is made of $CaCO_3$ with presence of various oxides depending on the zone where it was formed.

Table 1: Density of the analyzed materials.

Material	Density (g/cm^3)
White Concrete	0.571
Roman Brick NS	1.516
Roman Brick S	1.718
Refractory White	1.867
Refractory Red	1.944
Travertine	2.464

2.1 Average Absorption Cross Section

The RC used to perform the materials characterization has a volume of 0.08 m^3 and is of cylindrical shape. Figure 1 and Figure 2 show the experimental setup. The resonance frequency of the fundamental mode is f_0=833.7 MHz, giving a lowest usable frequency (LUF) of about $5f_0$=4168 MHz. A vertical stirrer is placed inside the chamber. The stirrer has Z-folded shape with copper paddles: the bottom part has height of 17 cm and width of 13 cm, while the upper part has height of 17 cm and width of 6 cm. The stirrer is moved in a stepped (tuned) mode [22] by a stepper motor, which assures a 0.5-degree resolution. The transmitting and receiving antennas are two (A-Info) working between 50 GHz and 70 GHz. A Vector Network Analyzer (VNA − Anritsu Model MS4647B) is used to measure the transmission coefficient between the two antennas, while they operate inside the chamber, both in presence and in absence of the sample. As VNA settings, the measurement registration has step of 20 MHz, a 1000 Hz IF bandwidth has been selected for noise reduction and a 5 seconds sweep time has been set for each range. By this way, a sufficient frequency resolution (1.25 MHz) can be reached to allow for a good electronic stirring / moving frequency averaging [23]. The measurements are first performed at 180 uncorrelated stirrer positions (2 degrees steps) and then used to obtain the empty RC average quality factor. Then, the absorbing material sample is placed over a polystyrene foam support inside the RC, and the mechanical stirring procedure repeated over 180 stirring positions to obtain the Q of the loaded RC.

The RC is an overmoded cavity where wave mixing occurs and is accompanied by strong field fluctuations driven by the movement of the mechanical stirrer. Therefore, besides Q, also the ACS has to be averaged over the 180 stirrer positions. In particular, the average ACS is defined as [24]

$$ACS = \frac{\langle P_s \rangle}{S_i} \tag{1}$$

where P_s is the power dissipated by the sample and $S_i = <|E_T^2|>/\eta_0$ is the incident scalar power density, whereas the bracket symbol <•> means either an ensemble average over the stirrer rotation and frequency stirring, η_0 is the free space wave impedance, and $|E_T|$ is the total field magnitude. In (1), idealized field uniformity, anisotropy, and uncorrelation are assumed: consequently, the statistical distribution of the transmission coefficient S_{21} approaches the asymptotic distribution χ_2 (chi-distribution with 2 degrees of freedom) [25-28]. The spectral characteristics of a mode-stirred cavity are sensible to energy perturbations, e.g. a low-loss dielectric inclusion, because of the strong modal overlapping occurring in the over-moded regime. The total losses inside an RC are due to different loss mechanisms through walls, antennas and material samples. Indicated as Q_u the quality factor measured without the material sample, and as Q_l the one after the sample allocation inside the RC, the contribution Q_s due to the material dissipation only can be easily evaluated by the differential measurement [13]

$$Q_s^{-1} = Q_l^{-1} - Q_u^{-1} \tag{2}$$

In terms of stored energy and dissipated power:

$$Q_s = \frac{\omega W}{< P_s >} = \frac{\omega\, S_i V}{c < P_s >} \tag{3}$$

where ω is the angular frequency of excitation, W the energy stored by the chamber, V the chamber volume, and c the speed of light in vacuum. By substituting (1) into (3) and unfolding, yields

$$ACS = \frac{\omega W}{c Q_s} = \frac{2\pi V}{\lambda Q_s} \tag{4}$$

where λ is the wavelength at the operation frequency of the RC. The indirect ACS estimation can be achieved by S_{21} (with and without the material sample) through the well-known relation

$$Q = \frac{16\pi^2 V < P_r >}{\lambda^3 \eta_{Tx} \eta_{Rx} < P_t >} \quad \text{or} \quad Q = \frac{16\pi^2 V < |S_{21}|^2 >}{\lambda^3 \eta_{Tx} \eta_{Rx}} \tag{5}$$

where $<|S_{21}|^2>$ is the average insertion loss − i.e. the rate $< P_r >/< P_t >$, where P_r is the power captured by the receiving antenna R_x with total radiation efficiency $\eta_{Rx} = 1-|<S_{22}>|^2$ and P_t is the power injected by the transmitting antenna T_x with total radiation efficiency $\eta_{Tx} = 1-|<S_{11}>|^2$ − and S_{21} is the transmission scattering parameter between VNA port 1, connected to T_x, and port 2, connected to R_x. As shown in (5), the calibration has been performed by taking into account all the impedance mismatch effects due to cable, antennas, connectors, and proximity. In particular, the reflection coefficient of the antennas has been taken into account in Q and ACS computation [11].

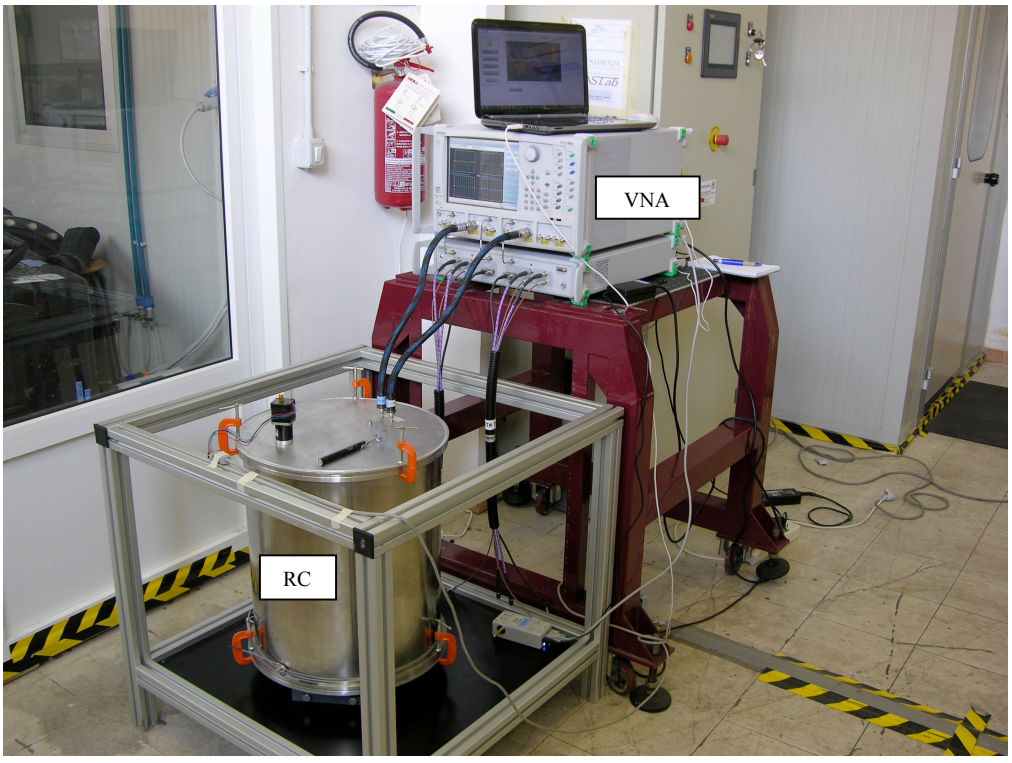

Fig. 1. VNA connected to Reverberation Chamber.

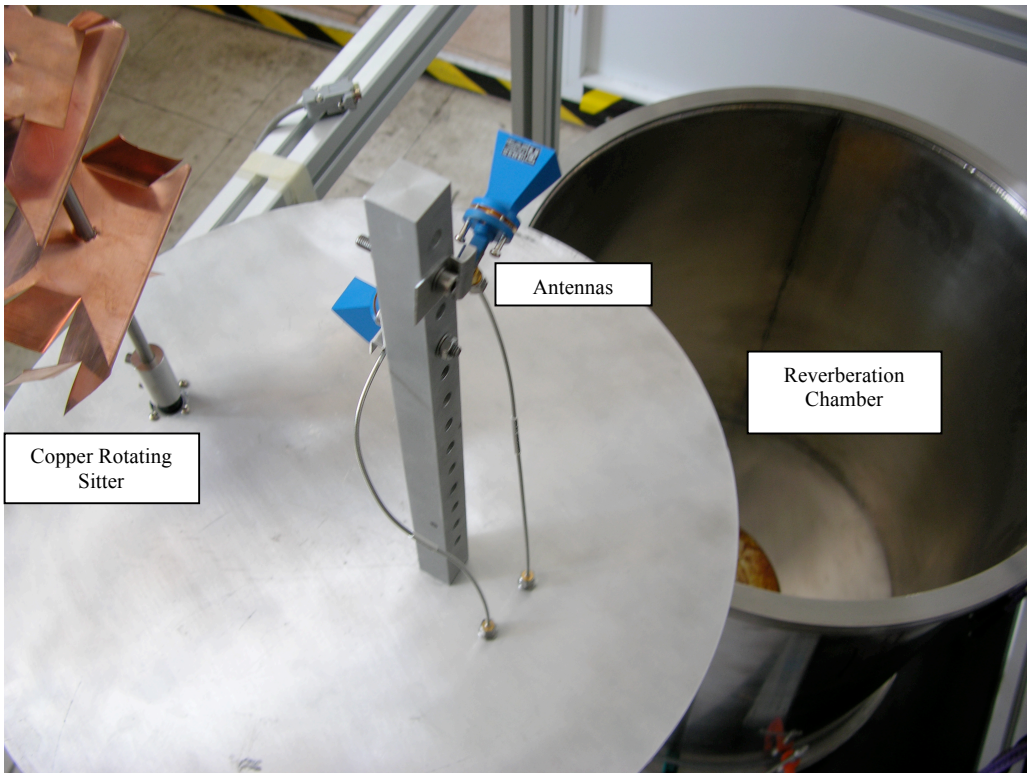

Fig. 2. Reverberation chamber: two horn antennas type XB-HA15-20 working in the frequency range 50-70 GHz and copper rotating stirrer.

3 RESULTS AND DISCUSSION

Before testing the building samples, we made sure that the 180 stirrer positions are statistically uncorrelated – meaning that they are able to effectively change the cavity boundary conditions, thus creating new sets of modes to foster wave field mixing. In a conventional RC operated at microwave regimes (~ up to 10 GHz), a 1° angular step size is typically used in ACS experiments. However, there is a limited scientific literature on the operation of an RC at mmWave frequencies [29,30]. We calculate the correlation coefficient between stir traces in a range of angles between 0.5 and 2 degrees. In particular,

$$\rho_{a,b} = \frac{\sum_{n=1}^{N}\left(Q_{a,n} - \overline{Q_a}\right)\left(Q_{b,n} - \overline{Q_b}\right)}{\sqrt{\sum_{n=1}^{N}\left(Q_{a,n} - \overline{Q_a}\right)^2 \sum_{n=1}^{N}\left(Q_{b,n} - \overline{Q_b}\right)^2}} \tag{6}$$

where N is the number of field samples used to calculate the coefficient between position *a* and *b*.

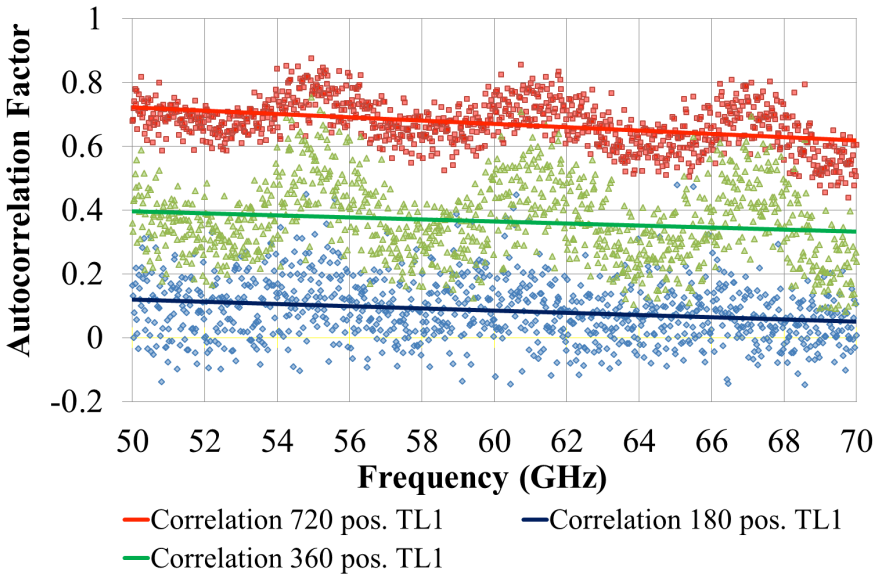

(a)

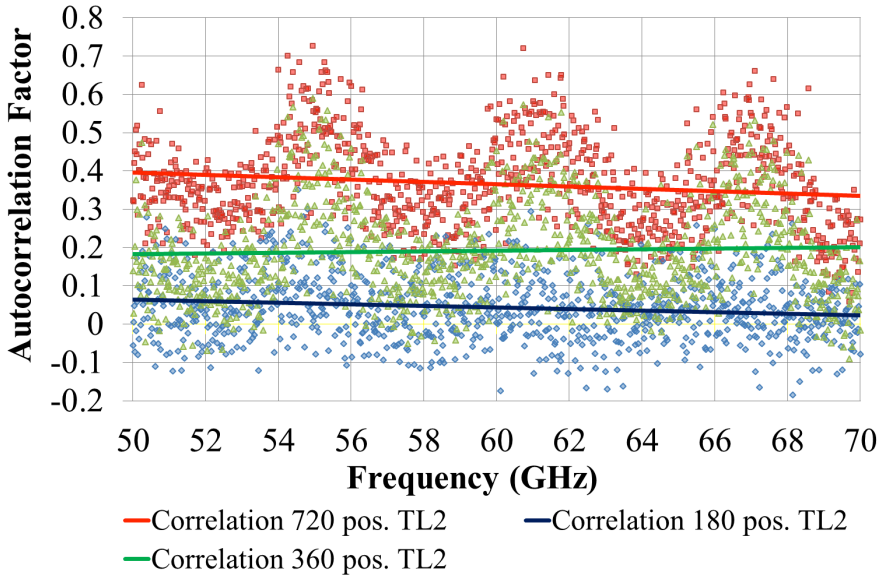

(b)

Fig. 3. Correlation factor TL1 (a) and TL2 (b) of Roman Brick S, as a function of the rotating stirrer angular step of 0.5° (720 pos.), 1°(360 pos.), and 2°(180 pos.).

Calculating the correlation between stir traces is important in reverberation chamber to assess the field mixing and the effectiveness of the stirrer. The correlation is calculated between original and shifted stir traces. In Fig.3 the Time Lag (TL) is plotted in frequency for three different stirrer angular step. Such factor represents the shift between stir traces, i.e., fields sampled collected at a specific point for a specific frequency are shifted of TL data samples: "a" and "b" in (6) are the data sets which the correlation is calculated from, so they are statistical variables [9,31]. In this case "a" and "b" are the data sets given by the chosen Time Lag, TL1 or TL2, i.e., for the generic lag k, they represent data set with the latest Q-k observations versus the first Q-k observations, considering Q the total amount of data. For instance, considering 180 stirring positions, if k=1 the first Q-1 values are correlated to the latest Q-1 ones, i.e. Q_1 ... Q_{179} versus Q_2 ... Q_{180} . For k=2, the first Q-2 values are correlated to the latest Q-2, i.e. Q_1 ... Q_{178} versus Q_3 .... Q_{180} , and so on. In (6) the summation limit N is so given by Q-k.

If the correlation values are close to 1 then the angular step size could be relaxed without loss of chamber sensitivity. On the contrary, if the correlation values are close to zero then a small step size is required to increase the RC sensitivity at these frequencies. Results in Fig. 3 show that the correlation coefficient becomes lower than the empirical threshold *1/e* when the angular step is between 1 and 2 degrees, so a stirrer step of 2 degrees (180 positions) turns out to be a safe choice. In our measurements we observed an oscillating behavior of the correlation function in frequency that is much evident with the increase of angular positions. This behavior is currently under investigation.

In Figure 4 and Figure 5 the results obtained for the Q factor and ACS are plotted. The thick lines are obtained as ensemble average of the thin (shaded) lines: this is a usual procedure to mitigate the large spectral variability of reverberation chamber measurements [10]. Figure 4 shows the average quality factors of the RC both when loaded and unloaded with material samples, as well as with and without the polystyrene sample holder inside the RC working volume. Also, the quality factor in presence of a sample with water is shown. The dynamic range of the measurement is set between unloaded RC and loaded RC with water. In presence of water, the Q values are lower than in presence of the test samples (around 3200), the empty RC has much higher Q values (around 17000): this is a clear indication that the measurement set-up offers enough dynamic range to properly quantify the ACS of the building material samples under test.

The Q of the investigated material samples is highlighted in Figure 4 (b) as compared against water, which shows a consistent trend over the investigated frequency range. In particular, the Q values increase at frequencies between 50 GHz and 53 GHz, and then are almost flat until 63 GHz. At higher frequencies,

the quality factor decreases until 66.5 GHz and increases again until 68 GHz. All the Q values fall within the range from 4000 to 5750.

Figure 5 shows the ACS values for all the investigated material samples. Interestingly, the samples show an almost flat ACS between 53 and 63 GHz, as anticipated by the Q measurements. The large scale frequency behavior of the ACS of cubic samples has a U-profile: whether this effect can be ascribed to the sample shape – the cylindrical sample with water has different profile – or to the specific characteristics of the RC facility [32,33], needs to be further investigated and clarified. Fine scale frequency fluctuations encode the material behavior, and their dependence on the chemical composition is also an interesting issue to be investigated. The material density values in Table 1 have a clear correlation with the quality factor and ACS measurements: the higher the density, the higher the Q and the lower the ACS, since more compact materials increase the material reflectivity, while less dense materials have greater absorption. Such qualitative explanation is confirmed both for Refractory Red and Refractory White, as materials with the same chemical composition present different values because of their density; the same findings are obtained for Roman Brick S and NS. Travertino presents the lowest values of ACS and has the highest density. The sample made of White Concrete, instead, presents a special behavior: it has the lower density, thus a very low Q factor should be expected. Conversely, the Q values measured suggest that the chemical components play a more important role than the density do for such material at mmWave: the presence of Aluminum powder, in fact, can improve the reflectiveness of the material and delimit the effect of the low density. Moreover, considering the chemical composition, Refractory bricks, which includes Alumina and Silica, presents ACS values higher than or equal to those of Roman Bricks: such result is due to the presence of metallic components, which improve the reflectiveness. Finally, also the surface roughness plays an important role: from the plots in Figure 4 it can be appreciated that the Refractory White, that is less smooth than the Roman Brick S, presents quite the same properties of the Roman Brick S, even if it has higher density and metallic inclusions in its chemical composition.

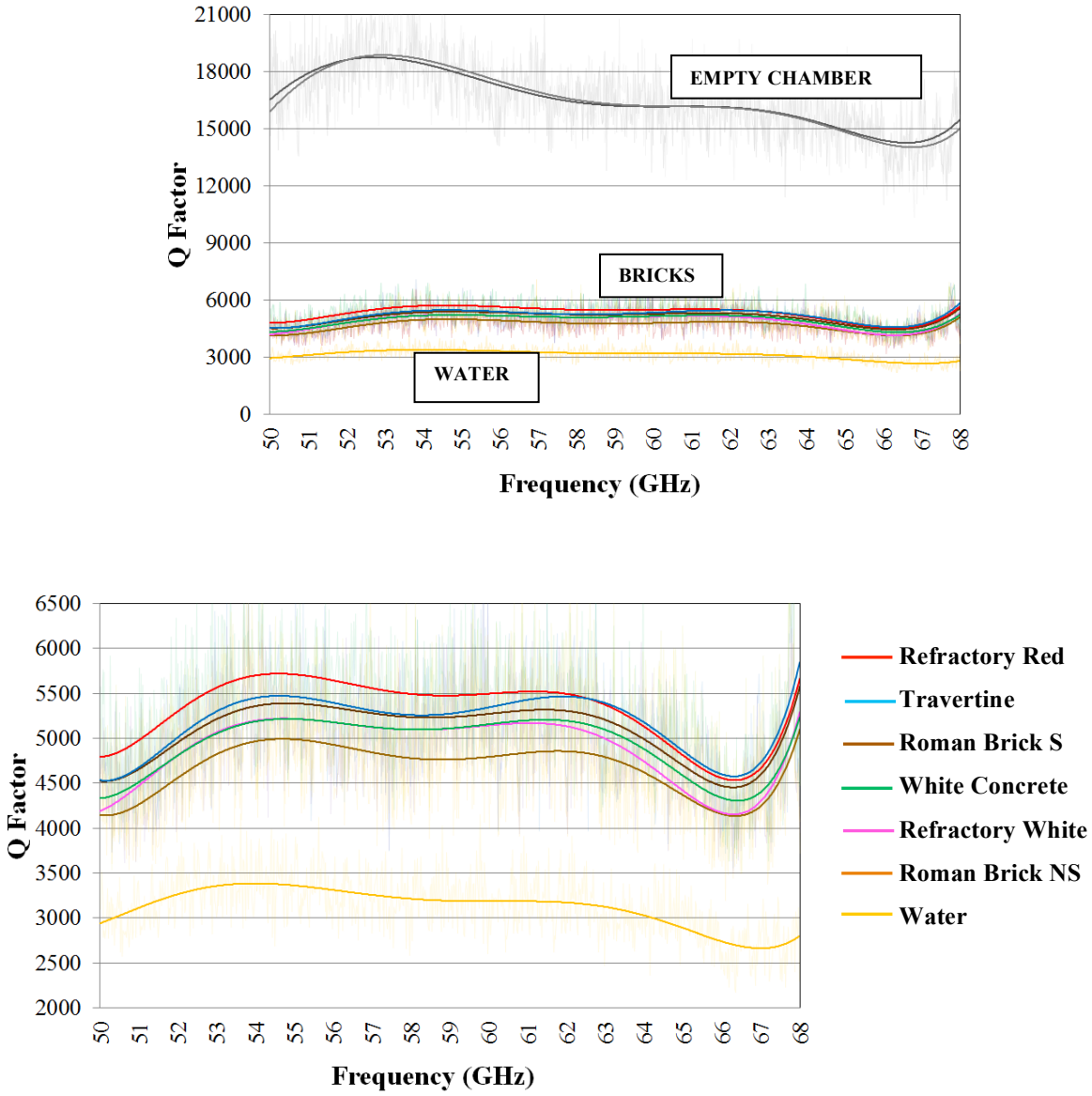

Fig. 4. Q factor of materials-loaded and empty Chamber. In (a) the difference between empty chamber and sample loading condition; in (b) enlargement of loaded condition only.

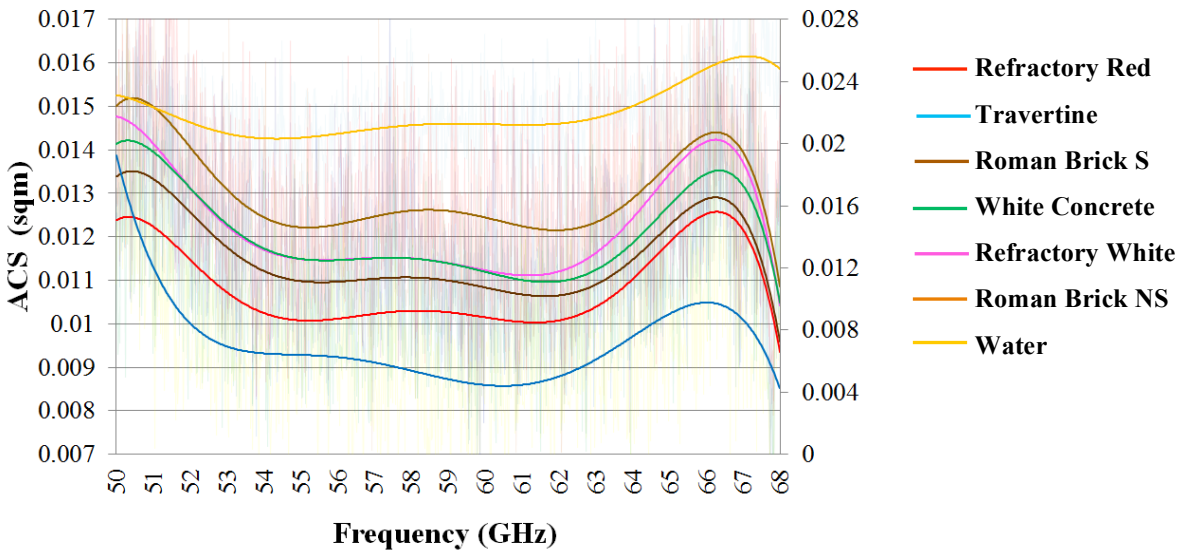

Fig. 5 ACS of the tested materials (the water values is shown in the scale on the right).

4 CONCLUSIONS

Reverberation chamber measurements of an average absorption cross section have been performed at mm Wave regime for selected building materials. Both the quality factor and the absorption cross-section of cubic material samples have been obtained through the reverberation chamber method. The observed frequency behavior is almost flat over a wide frequency band from 53 to 63 GHz. Further investigations are necessary to relate large- and fine-scale frequency fluctuations to both the sample shape and the chemical composition of materials. Ongoing research is devoted to the investigation of the effects of the surface roughness and shape, as well as of the RC test fixture, on the absorption cross section, in order to better characterize arbitrary materials at very high frequencies.

ACKNOWLEDGMENT

Financial support from Telecom Italia Lab (GRANT NUMBERS: 5003326289 – Sapienza University of Rome, Italy; 5003355778 – University of Nottingham, United Kingdom) is gratefully acknowledged.

REFERENCES

[1] Rappaport TS, Gutierrez F, Ben-Dor E, Murdock J N, Qiao Y, Tamir J I, 2013 Broadband millimeter-wave propagation measurements and models using adaptive-beam antennas for outdoor urban cellular communications *IEEE T. Ant. Propag.* **61** 1850−9

[2] Rappaport T S, Sun S, Mayzus R, Zhao H, Azar Y, Wang K, Wong G N, Schulz J K, Samimi M, Gutierrez F, 2013 Millimeter wave mobile communications for 5G cellular: it will work! *IEEE Access* **1** 335−49

[3] Yang H S, Ma J, Lu Z-Z, 1995 Circular groove guide for short millimeter and submillimeter waves *IEEE T. Microw. Theory* **43** 324−30

[4] Afsar M N, Ding H, Tourshan K, 1999 A new 60 GHz open-resonator technique for precision permittivity and loss-tangent measurement *IEEE T. Instr. Meas.* **48** 626−30

[5] Afsar M N, Ding H, 2001 A novel open-resonator system for precision measurement of permittivity and loss-tangent *IEEE T. Instr. Meas.* **50** 402−5

[6] Tischer F J, 1963 The groove guide, a low loss waveguide for millimeter waves *IEEE T. Microw. Theory* **11** 291−6

[7] Afsar M N, 1984 Dielectric measurement of millimiter-wave materials *IEEE T. Microw. Theory* **32** 1598−609

[8] Vakili I, Ohlsson L, Wernersson L-E, Gustafsson M, 2015 Time-domain system for millimeter-wave material characterization *IEEE T. Microw. Theory* **63** 2915−22

[9] IEC 61000-4-21 Standard, 2011, Electromagnetic compatibility (EMC) - Part 4-21: Testing and measurement techniques - Reverberation chamber test methods

[10] Hill D A, 1994 Electronic mode stirring for reverberation chambers *IEEE T. Electromagn. Comp.* **36** 294−9

[11] Besnier P, Lemoine C, Sol J, 2015 Various estimations of composite Q-factor with antennas in a reverberation chamber *IEEE International Symposium on Electromagnetic Compatibility*, pp. 1223−7

[12] Hallbjörner P, Carlberg U, Madsén K, Andersson J, 2005 Extracting electrical material parameters of electrically large dielectric objects from reverberation chamber measurements of absorption cross section *IEEE T. Electromagn. Comp*. **47** 291−303

[13] Gradoni G, Micheli D, Moglie F, Mariani Primiani V, 2012 Absorbing cross section in reverberation chamber: experimental and numerical results *Prog. Electromagn. Res. B* **45** 187−202

[14] Micheli D, Barazzetta M, Moglie F, Mariani Primiani V, 2015 Power boosting and compensation during OTA testing of a real 4G LTE base station in reverberation chamber IEEE T. Electromagn. Comp. **57** 623−34

[15] Micheli D, Vricella A, Pastore R, Delfini A, Giusti A, Albano M, Marchetti M, Moglie F, Mariani Primiani V, 2016 Ballistic and electromagnetic shielding behaviour of multifunctional Kevlar fiber reinforced epoxy composites modified by carbon nanotubes *Carbon* **104** 141−56

[16] Micheli D, Vricella A, Pastore R, Delfini A, Bueno Morles R, Marchetti M, Santoni F, Bastianelli L, Moglie F, Mariani Primiani V, Corinaldesi V, Mazzoli A, Donnini J, 2017 Electromagnetic properties of carbon nanotube reinforced concrete composites for frequency selective shielding structures *Constr. Build. Mat.* **131** 267−77

[17] Cozza A, 2011 The role of losses in the definition of the overmoded condition for reverberation chambers and their statistics 2011 *IEEE T. Electromagn. Comp*. **53** 296−307

[18] Amador E, Lemoine C, Besnier P, Laisné A, 2010 Reverberation chamber modeling based on image theory: investigation in the pulse regime *IEEE T. Electromagn. Comp.* **52** 778−89

[19] Gradoni G, Yeh J-H, Xiao B, Antonsen T M, Anlage S M, Ott E, 2014 Predicting the statistics of wave transport through chaotic cavities by the random coupling model: a review and recent progress *Wave Motion* **51** 606−21

[20] Arnaut L R, 2003 Statistics of the quality factor of a rectangular reverberation chamber *IEEE T. Electromagn. Comp.* **45** 61−76

[21] Arnaut L R, Gradoni G, 2013 Probability distribution of the quality factor of a mode-stirred reverberation chamber *IEEE T. Electromagn. Comp.* **55** 35−44

[22] Corona P, Ladbury J, Latmiral G, 2002 Reverberation-chamber research-then and now: a review of early work and comparison with current understanding *IEEE T. Electromagn. Comp.* **44** 87-94

[23] Madsen K, Hallbjorner P, Orlenius C, 2004 Models for the number of independent samples in reverberation chamber measurements with mechanical, frequency, and combined stirring *IEEE Ant. Wireless Propag. Lett*. **3** 48−51

[24] IEC 61000-4-21: Electromagnetic Compatibility (EMC) – Part 4-1:Testing and measurement techniques – Reverberation chamber test methods. *IEC Standard* 77B/576/CD 2009

[25] Sorrentino A, Mascolo L, Ferrara G, Migliaccio M, 2012 The fractal nature of the electromagnetic field within a reverberating chamber *Prog. Electromagn. Res. C* **27** 157−67
[26] Moglie F, Mariani Primiani V, 2011 Analysis of the independent positions of reverberation chamber stirrers as a function of their operating conditions *IEEE T. Electromagn. Comp.* **53** 288−95
[27] Moglie F, Mariani Primiani V, 2012 Numerical analysis of a new location for the working volume inside a reverberation chamber *IEEE T. Electromagn. Comp*. **54** 238−45
[28] Hong J-I, Huh C-S, 2010 Optimization of stirrer with various parameters in reverberation chamber 2010 *Prog. Electromagn. Res*. **104** 15−30
[29] Fall A K, Besnier P, Lemoine C, Zhadobov M, Sauleau R, 2015 Design and experimental validation of a mode-stirred reverberation chamber at millimeter waves *IEEE T. Electromagn. Comp*. **57** 12-21
[30] Senic D, Remley K A, Wang C-M J, Williams D F, 2016 Estimating and reducing uncertainty in reverberation-chamber characterization at millimeter-wave frequencies *IEEE T. Ant. Propag*. **64** 3130−40
[31] Papoulis A, Unnikrishna Pillai S, 2015 Probability, random variables and stochastic processes, 4th ed. McGraw-Hill
[32] Amador E, Andries M I, Lemoine C, Besnier P, 2011 Absorbing material characterization in a reverberation chamber *Proc. 10th Int. Symp. Electromagn. Comp.*, pp. 117−22
[33] Andries M I, Besnier P, Lemoine C, 2012 On the prediction of the average absorbing cross section of materials from coherence bandwidth measurements in reverberation chamber *Int. Symp. Electromagn. Comp.*, pp. 1-6